THE STUDY OF GLOBAL STABILITY AND SENSITIVE ANALYSIS OF HIGH PERFORMANCE AIRCRAFT AT HIGH ANGLES-OF-ATTACK

H. Gao, Z. D. He and Z. Q. Zhou
Northwestern Polytechnical University
Xian Shaanxi Province
People's Republic of China

Abstract

In this paper, the qualitative theory of differential equations is used to study the global stability of high performance aircraft.

The relations between the stability criteria commonly used in aircraft design, such as $Cn_\beta dyn.$ and LCDP etc., and eigenvalues of the linearized matrices at the equilibrium points are discussed . It is believed that these criteria can be deduced from the linearized matrices of the aircraft nonlinear dynamic system at a specific flight state, therefore, they can only predict the local stability of an aircraft at high angles-of-attack. And then, sensitivity analysis is used to study the effects of cross-coupling derivatives and acceleration derivatives on aircraft response. Those derivatives occur when angles-of-attack are high. According to the calculated results, we find that the lateral moment derivatives due to pitch, such as Cn_α, $Cn_{\dot\alpha}$, Cl_α, $Cl_{\dot\alpha}$ may cause strong effects on stability. Especially, $Cn_\alpha$and $Cn_{\dot\alpha}$ cause two typical unstable motions of the aircraft.

For modern fighter, flight at high angles-of-attack is an inherent part of maneuvering. Typical modern fighter aircraft achieves maximum lift at angles of attack from approximately 25° to 35°. Aggressive maneuvering can cause pitch overshoots and angles of attack transient to 60 and therefore are subjected to conditions where the flow becomes highly asymmetric, at which we will face the problems about aircraft dynamic unstabilities.

During the past two decades, due to the development of the wind tunnel testing, radio-control flight testing, flight testing and flight simulation skills, the instabilities at high angles-of-attack have been understood further and some criteria for predicting departure characteristics and spin susceptibility, such as, directional departure parameter $Cn_\beta dyn.$, lateral control departure parameter LCDP and couple criteria etc. used in preliminary designs, have been set up. However, the aeroforces and moments at high angles-of-attack are severely nonlinear and the amplitudes of the motion parameters change rapidly, therefore, the nonlinear dynamic equations of the aircraft must be used to describe the aircraft's motion. In the past time, most of early research work is based on steady state assumption and linearization on which only limited and localized information regarding aircraft behaviors at high angles-of-attack is available.

At the end of seventies , a few of flight dynamicists applied qualitative theory of O.D.E., bifurcation and catastrophe theories to analysing the global stabilities of the complicated nonlinear dynamic equations of the aircraft.[1] According to these theories, we have discovered in this paper the relations between stability bounds determined by these theories and those commonly used criteria. As an example, the relations between global behaviors and several typical high angles-of-attack phenomena of a sample aircraft are analysed.

Furthermore, in order to analyse the effects of separate and asymmetrical flow, by adding some of the cross-coupling derivatives or angular acceleration derivatives and by comparing the time history with and without these terms, the sensitivity of aircraft response to these terms can be clearly observed.

The Global Stability Analysis of Aircraft's Flight at High Angles-of-Attack

The nonlinear ordinary differential equations describing the aircraft's motions at high angles-of-attack can be written concisely as follow :

$$\dot{X}=F(X,C) \qquad (1)$$

where X is a column of state vector, C is a column of control vector. The equilibrium surfaces are governed by

$$F(X,C)=0 \qquad (2)$$

According to O.D.E. qualitative theory, in order to discuss the stability of eq.(1), first, we should analyse the stability in the neighborhood of the state variables determined by eq.(2), which presents the reference condition of steady flight and the stability is called local stability. The column of state vectors and control vectors X, C, whose values satisfy eq.(2) , are called equilibrium points . Because of the nonlinear behaviors of the dynamic systems, their stabilities probably have structural changes while control vector varies. For example, the bifurcation points,

catastrophe points and periodic attractors etc. may be produced from the equilibrium points. Hence, in nonlinear systems the stability must be analysed not only in the neighborhood of equilibrium points, but also in the probable spaces of state and control vectors. The latter is called the global stability.

We discuss the application of these theories to analysing the dynamic behaviors of the aircraft at high angles-of-attack as follows.

The Aircraft Motion Equations

Suppose the aircraft is a rigid body and the engine gyroscopic moments can be neglected .

Dynamic equations are :

$$\dot{\alpha} = q + [-(\frac{\bar{q}S}{mV} C_x - \frac{g}{V}\sin\theta + r\sin\beta)\sin\alpha + (\frac{\bar{q}S}{mV} C_z + \frac{g}{V}\cos\theta\cos\phi - p\sin\beta)\cos\alpha]\sec\beta \quad (3)$$

$$\dot{\beta} = -[(\frac{\bar{q}S}{mV} C_x - \frac{g}{V}\sin\theta)\sin\beta + r]\cos\alpha + (\frac{\bar{q}S}{mV} C_y + \frac{g}{V}\cos\theta\sin\phi)\cos\beta - [(\frac{\bar{q}S}{mV} C_z + \frac{g}{V}\cos\theta\cos\phi)\sin\beta - p]\sin\alpha \quad (4)$$

$$\dot{p} = [-(\frac{I_z - I_y}{I_x} + \frac{I_{xz}^2}{I_x I_z}) qr + (1 - \frac{I_y - I_x}{I_z})\frac{I_{xz}}{I_x} pq + \frac{\bar{q}Sb}{I_x}(C_l + \frac{I_{xz}}{I_z} C_n)]/(1 - \frac{I_{xz}^2}{I_x I_z}) \quad (5)$$

$$\dot{q} = \frac{\bar{q}S\bar{C}}{I_y} C_m + \frac{I_z - I_x}{I_y} pr + \frac{I_{xz}}{I_y}(r^2 - p^2) \quad (6)$$

$$\dot{r} = [(\frac{I_{xz}^2}{I_x I_z} - \frac{I_y - I_x}{I_z}) pq + (1 + \frac{I_z - I_y}{I_x})\frac{I_{xz}}{I_z} qr + \frac{\bar{q}Sb}{I_z}(\frac{I_{xz}}{I_x} C_l + C_n)]/(1 - \frac{I_{xz}^2}{I_x I_z}) \quad (7)$$

The variation of the aircraft velocity at high angles-of-attack can be neglected, so, the velocity equation and the terms concerned with thrust are abandoned. Kinematical equations are :

$$\dot{\theta} = q\cos\phi - r\sin\phi \quad (8)$$

$$\dot{\phi} = p + qtg\theta\sin\phi + rtg\theta\cos\phi \quad (9)$$

$$\dot{\psi} = q\sin\phi\sec\theta + r\cos\phi\sec\theta \quad (10)$$

Eq.(8) and (9) decouple with dynamic equations if the gravity terms are not involved. The calculation experiences show that the gravity terms don't affect the values and the shapes of equilibrium surfaces seriously except the flat spin region.

In order to calculate the trails of aircraft gravity center in spin, the velocities in earth-fixed axis are introduced. The formulae are:

$$\dot{X} = V(A\cos\psi - B\sin\psi) \quad (11)$$

$$\dot{Y} = V(A\sin\psi + B\cos\psi) \quad (12)$$

$$\dot{Z} = V[\cos\theta(\sin\beta\sin\psi + \cos\beta\sin\alpha\cos\phi) - \cos\beta\cos\alpha\sin\theta] \quad (13)$$

where

$$A = \cos\beta\cos\alpha\cos\theta + \sin\theta(\sin\beta\sin\phi + \cos\beta\sin\alpha\cos\phi) \quad (14)$$

$$B = \sin\beta\cos\phi - \cos\beta\sin\alpha\sin\phi \quad (15)$$

The Models of the Aerodynamic Coefficients

The aerodynamic force and moment coefficients at high angles-of-attack are complicated functions of several state variables . Even though they are given in the form of aerodynamic derivatives for simplifying the calculations. They are the two dimensional functions of and . The formulae are:

$$C_x = C_x(\alpha, \beta, \vec{\delta}=0) + C_{x\delta e}(\alpha,\beta)\delta e \quad (16)$$

$$C_y = C_y(\alpha, \beta, \vec{\delta}=0) + C_{y\delta e}(\alpha,\beta)\delta e + C_{y\delta a}(\alpha,\beta)\delta a + C_{y\delta r}(\alpha,\beta)\delta r + \frac{b}{2V}[C_{yp}(\alpha)p + C_{yr}(\alpha)r] \quad (17)$$

$$C_z = C_z(\alpha, \beta, \vec{\delta}=0) + C_{z\delta e}(\alpha,\beta)\delta e \quad (18)$$

$$C_l = C_l(\alpha, \beta, \vec{\delta}=0) + C_{l\delta e}(\alpha,\beta)\delta e + C_{l\delta a}(\alpha,\beta)\delta a + C_{l\delta r}(\alpha,\beta)\delta r + (\frac{b}{2V})[C_{lp}(\alpha)p + C_{lr}(\alpha)r + C_{l\dot{\beta}}\dot{\beta}] + C_{l\alpha}(\alpha - \alpha_T) + (\frac{\bar{C}}{2V})[C_{l\dot{\alpha}}\dot{\alpha} + C_{lq}q] \quad (19)$$

$$C_m = C_m(\alpha,\beta) + C_{m\delta e}(\alpha,\beta)\delta e + (\frac{\bar{C}}{2V})C_{mq}(\alpha)q + \frac{b}{2V}(C_{m\dot{\beta}}\dot{\beta} + C_{mp}p + C_{mr}r) \quad (20)$$

$$C_n = C_n(\alpha, \beta, \vec{\delta}=0) + C_{n\delta e}(\alpha,\beta)\delta e + C_{n\delta a}(\alpha,\beta)\delta a + C_{n\delta r}(\alpha,\beta)\delta r + (\frac{b}{2V})[C_{np}(\alpha)p + C_{nr}(\alpha)r + C_{n\dot{\beta}}\dot{\beta}] + C_{n\alpha}(\alpha - \alpha_T) + (\frac{\bar{C}}{2V})(C_{nq}q + C_{n\dot{\alpha}}\dot{\alpha}) \quad (21)$$

where $\dot{\delta}=0$ means $\delta_a=\delta_e=\delta_r=0$

The coefficients are generally given in the form of discrete points. So, the relations between the high angles-of-attack aerodynamic coefficients and state variables are presented in tables , the derivatives are calculated by using bi-cubic spline method.

The Relations between Equilibrium Points and the Criteria for Predicting Departure Characteristics and Spin Susceptibility

According to O.D.E. qualitative theory, the local stability in the neighborhood of equilibrium points are generally determined by the eigenvalues of the matrix of the linearized derivative operator. With the aircraft motion equations (3) up to (5) , neglecting inertia product, aerodynamic damping moments and cross moments, the following equations can easily be deduced:

$$\dot{\alpha}=q-(p\cos\alpha+r\sin\alpha)tg \qquad (22)$$

$$\dot{\beta}=p\sin\alpha-r\cos\alpha \qquad (23)$$

$$\dot{p}=\bar{L}_\alpha\alpha+\bar{L}_\beta\beta \qquad (24)$$

$$\dot{q}=\bar{M}_\alpha\alpha+\bar{M}_\beta\beta \qquad (25)$$

$$\dot{r}=\bar{N}_\alpha\alpha+\bar{N}_\beta\beta \qquad (26)$$

In condition of steady rectilinear flight ($p_e=q_e=r_e=0$), the characteristic equation of the matrix of the linearized derivative operator is

$$\Delta(S)=S(S^4+AS^2+B) \qquad (27)$$

In Eq.(27) , coefficients A and B are equal to the characteristic equation's coefficients determining couple criteria in ref.(6) . So , all couple criteria can be obtained from eq.(27) . Furthermore, in coefficient B, neglecting the terms concerned with L and N, the directional departure parameter $C_{n\beta dyn.}$ can be deduced. In the same way, removing the couple moment between longitudinal and lateral, adding the lateral moment caused by aileron deflection, the lateral control departure parameter LCDP can be deduced. This shows that the criteria can be obtained by variedly simplifying the models at equilibrium points. Because of no limits of undisturbed motion in eq.(3) up to (9) , the analysis of local stability by the eigenvalues of the derivative operator matrix is more comprehensive and perfect than that by these criteria. However, for the nonlinear system viewpoint, it is still not enough. The global stability must be analysed.

The calculation shows that the results gained by the criteria coincide with these by qualitative theory at certain angles-of-attack. Because of the simplicity of the criteria, they are still available to practice.

Examples and Analysis of the Results

As an example, the equilibrium surfaces and corresponding eigenvalues of a combat aircraft in subsonic, high angles-of-attack flight have been calculated. At same time, the time histories of some special equilibrium points are computed. All original data of the aircraft are taken from ref.(2). Following illustrations show how to relate these special points with high angles-of-attack flight phenomena.

Wing Rock Fig.1(1) up to 1(5) present the equilibrium surfaces, in which the sample aircraft flies at V=118 m/s H=10 km, $\delta_a=\delta_r=0$, and the control variable δe changes from 0° to -27°.The characteristics of roll, pitch and yaw rates in the figures represent the results of nonlinear models. The eigenvalues of the matrix of the linearized derivative operator at every equilibrium point are calculated. In the figures, the symbol S-S in the branch indicates that the real parts of the eigenvalues are all negative. The equilibrium points in the branch are locally stable. The symbol L-L indicates that there are a pair of conjugate complex eigenvalues of the matrix, whose real parts are positive, and the points are locally unstable with a divergent oscillation. These symbols give the stability around equilibrium points, but they can not indicate whether the state variables diverge continuously or converge to a periodic attractor ultimately and whether they are stable globally or not. In spite of this, studying each equilibrium point carefully can really provide further information about the aircraft nonlinear dynamic behaviors. Calculation

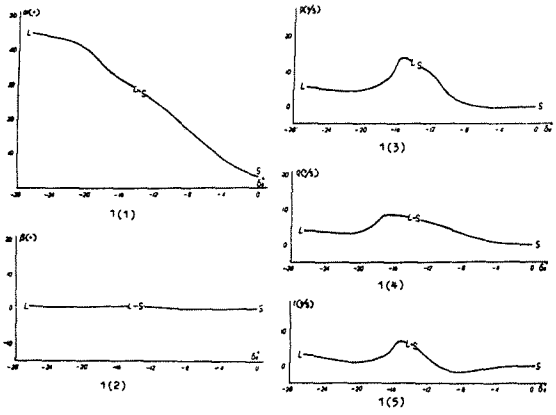

FIG.1(1) UP TO 1(5) THE EQUILIBRIUM SURFACE OF WING ROCK

experiences show that when the symbol at every equilibrium point changes from S to L , a periodic attractor will appear around the point.

In order to compare the results by criteria with those by the global analysis, the $Cn_{\beta}dyn.$ and LCDP are calculated at every equilibrium point in fig.1 . When δe changes from 0° to -15°, $Cn_{\beta}dyn.> 0$; when δe changes from 0° to -11°, LCDP > 0 . The trimmed angles-of-attack corresponding to -11° and -15° of the deflections of the elevator are about 22.5° and 30° respectively. The results by $Cn_{\beta}dyn.$ are much better coincidence with those by the global analysis in the example, but that probably is not generally correct. To know if a periodic attractor appears from S to L, the equilibrium point corresponding to $\delta e = -20.5^{\circ}$ in fig.1 is chosen to be an reference state

$(\alpha, \beta, p, q, r) =$

$(41^{\circ}, 0.4^{\circ}, 4.5^{\circ}/s, -1.4^{\circ}/s, 3.83^{\circ}/s)$

The units of angles and angle rates are degree and degree per second respectively. The law of the control surface deflections is

t(s)	0 ~5.0	5.0~6.1	6.1 ~23
δe	-20.5°	-10.5°	-20.5°

We can calculate the time histories of the aircraft motion as in fig.2(1) up to 2(5). In fig.2(1) upto 2(5) the response of the aircraft are violent and after 10 seconds the state variables begin to oscillate with 9 second period. Every state variable has its own regular variety, but all of them oscillate around the equilibrium point. The oscillation shows there is a periodic attractor exists.

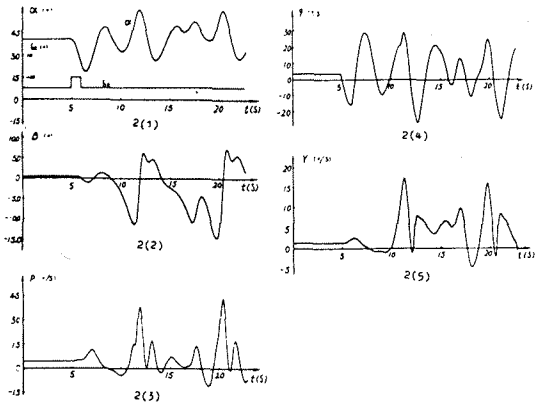

FIG.2(1) UP TO 2(5) THE TIME HISTORY OF WING ROCK

Spin Fig.3(1) up to 3(5) plots the equilibrium surfaces in which $\delta e=0^{\circ}$, $\delta a=15^{\circ}$ and δr changes from -34° to 30° . The angles-of-attack in the branch A-A are higher than 60°. The symbol L-L in the branch with the angles-of-attack lower than 35° has the same meaning as it in fig.1. If the gravity terms are neglected, the real parts of the eigenvalues in the branch with the angles-of-attack lower than 20° and δr changing from -15° to 15° are all negative. The symbol U in branch G-D indicates that there is an positive real eigenvalue at every equilibrium point, the point is locally unstable.

The points D and G are catastrophe points in fig.3(1) . The increase or decrease of the control variable around the catastrophe points cause the jump phenomenon.

There are L-L branch with 35° angles -of-attack and L-L branch with 65° one in the equilibrium surfaces of fig.3(1). The angles-of-attack corresponding to them greater than stall angle and the yaw rates are also big. So, around branch L-L and A-A, the existence of periodic attractors is probable. Furthermore, around the branch L-L in fig.3 , a steep spin occurs probably and at the branch A-A , a flat spin may occur.

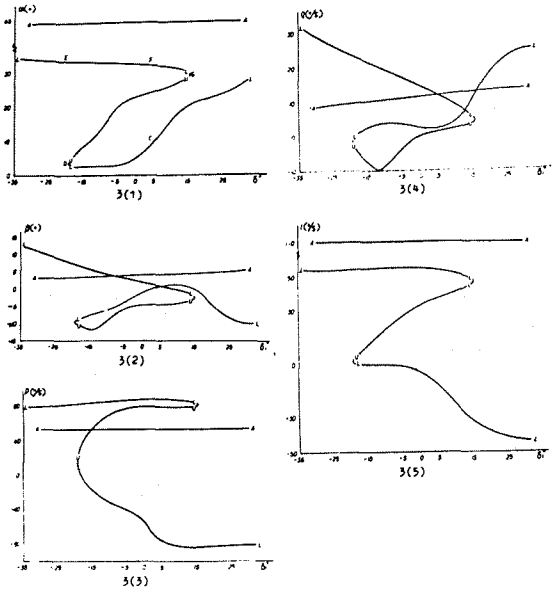

FIG.3(1) UP TO 3(5) THE EQUILIBRIUM SURFACE OF SPIN

In order to verify whether the phenomenon exists or not, the time histories of two equilibrium points at the branch A-A and L-L respectively are displayed. The initial values of state variables and control surfaces are at the branch L-L as following :

$(\alpha, \beta, p, q, r) =$

$(33.6^{\circ}, 9.6^{\circ}, 79^{\circ}/s, 26.7^{\circ}/s, 54.1^{\circ}/s)$

$(\delta a, \delta e, \delta r) = (15^\circ, 0^\circ, -26^\circ)$

The deflections of the three control surfaces do not vary throughout the process. The time histories are shown in fig.4(1) up to 4(6) .

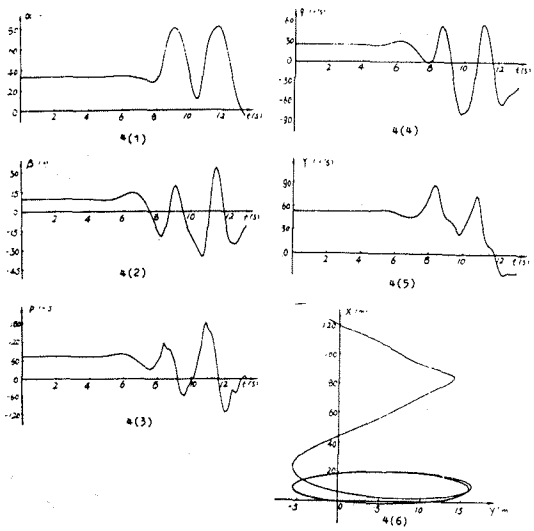

FIG.4(1) UP TO 4(6) THE TIME HISTORY OF THE STEEP SPIN

In the first 8 seconds, the aircraft maintains an angle higher than stall angle, large yaw and roll rates. The projection of the trial of centre of gravity is a circle of about 21 meter diameter. These features show that the equilibrium point is in the steep spin state. Then as the turbulence accumulates, the state variables begin to oscillate rapidly. Finally the computation is interrupted by the divergent angle of attack beyond the region of the data. The projection oscillates around the X-axis and is no longer a circle.

The initial state variables of next time history are at the branch A-A as following :

$(\alpha, \beta, p, q, r) = (64.1^\circ, 3.16^\circ, 53.1^\circ/s, 9.0^\circ/s, 110^\circ/s)$

The deflections of three control surfaces are:

$(\delta a, \delta e, \delta r) = (15^\circ, 0^\circ, -26^\circ)$

and they are unchanged during the time histories. The time histories are shown in fig.5(1) up to 5(3). Within the whole 35 seconds, all state variables change slightly and maintain very high angles-of-attack and yaw rate. That confirms that the dynamic balance has set up. Although the point is locally unstable, it diverges very slowly. The projection of the trial of centre of gravity in fig.5(3) is a circle with 3.2 meter diameter. Therefore, the aircraft is in the flat spin region.

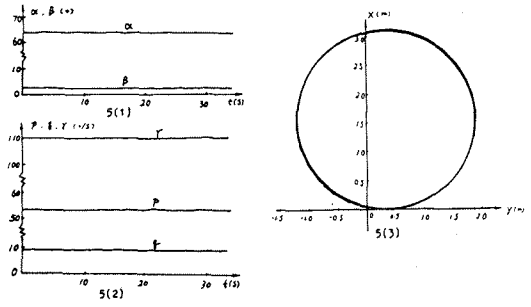

FIG.5(1) UP TO 5(3) THE TIME HISTORY OF THE FLAT SPIN

Sensitive Analysis

In this part of the paper, we try to ascertain whether the inclusion in the equations of motion of certain aerodynamic cross-coupling terms might be important for the stability of the aircraft at high-angles-of attack. A numerical study is undertaken in which the sensitivity of the motion time histories to these various terms is examined using the set of equations (3) to (13) on a digital computer.

In this case, the aerodynamic data in eq.(3)-(13) can be expressed in expressions (16)-(21). Some of the aerodynamic coefficients and derivatives which occur in expressions (16)-(21) are given in the computer program. Those are data for a typical modern fighter.

The other aerodynamic derivatives, including $C_{l\alpha}$, $C_{l\dot{\alpha}}$, C_{lq}, $C_{l\dot{\beta}}$, $C_{m\dot{\beta}}$, C_{mp}, C_{mr}, $C_{n\alpha}$, C_{nq}, $C_{n\dot{\alpha}}$, $C_{n\dot{\beta}}$ are cross-coupling or angular acceleration derivatives which exist at high angles - of-attack.

In some recent studies, these cross -coupling and angular acceleration derivatives were estimated or measured from the wind tunnel testing (ref.(8) to (15)). We assume the data as follow:

$C_{l\alpha} = \pm 0.05$ $\quad C_{l\dot{\alpha}} = \pm 0.5 \mp (\alpha - \alpha_T) \times 30.0$

$C_{lq} = \pm 0.5 \mp (\alpha - \alpha_T) \times 30.0$ $\quad C_{l\dot{\beta}} = -0.3$

$C_{n\alpha} = \pm 0.05$ $\quad C_{n\dot{\alpha}} = \pm 0.5 \mp (\alpha - \alpha_T) \times 60.0$

$C_{nq} = \pm 0.5 \mp (\alpha - \alpha_T) \times 60.0$ $\quad C_{n\dot{\beta}} = 0.6 - (\alpha - \alpha_T) \times 6.0$

$C_{mp} = -1.0$ $\quad C_{mr} = 0.1 - (\alpha - \alpha_T) \times 25.0$

$C_{m\dot{\beta}} = -0.1 - (\alpha - \alpha_T) \times 25.0$ (28)

In time history studies, we assume that these derivatives are added to the aerodynamic terms individually, but may also be added in combinations. The difference between time history responses obtained from with or without those particular derivatives or combinations determines the sensitivity

of the aircraft behaviour to the variation of those particular terms.

The aircraft is trimmed in a straight, level flight condition (n=1) with M =0.7, H = 15,400 m. At the moment t=0, a deflection angle $\Delta\delta_T$ =-8 is exerted. After that, all of the control devices are kept unchanged. With all the equations and data mentioned above, the aircraft response and time history of the parameters can be calculated, and a part of the results are presented in fig. 6 to fig. 7.

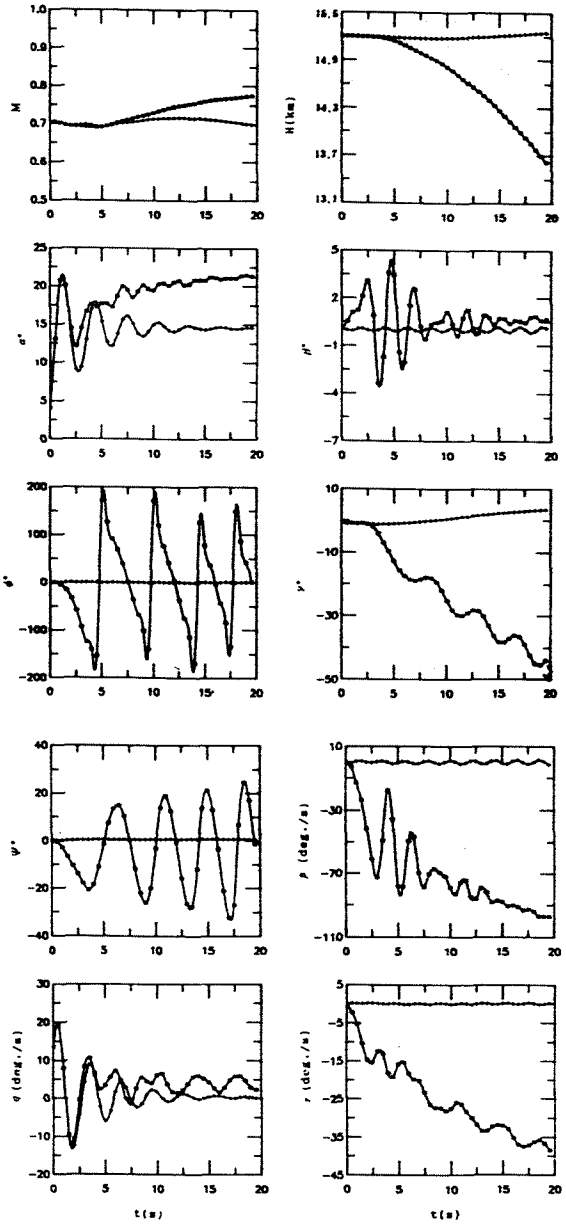

FIG. 6 THE EFFECTS OF Cn ON TIME HISTORY

It can be seen from the curves(with the symbols "+") in fig. 6 and 7, after deflection angle $\Delta\delta_T$ is exerted, an

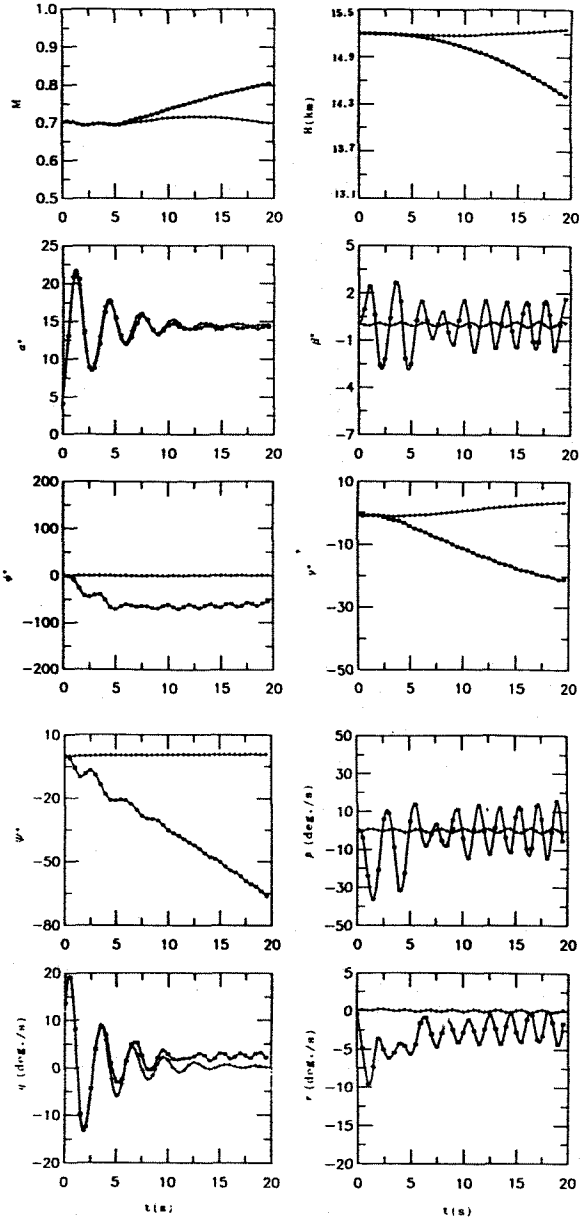

FIG. 7 THE EFFECTS OF Cn ON TIME HISTORY

oscillation of α occurs. The maximum value of α is about 21.5° . The oscillation is damped very fast and the aircraft almost reaches its new trimmed condition after 20 seconds later. In this process, the other parameters basically keep their original values.

Then the different cross-coupling and angular acceleration derivatives mentioned above are inserted into the loading equations. The results are presented in the curves (with the symbols ".") in fig.6 and fig.7.

Effects of $C_{n\alpha}$, $C_{n\dot{\alpha}}$, C_{nq} and $C_{n\dot{\beta}}$

From fig.6 we can see that the motion sensitivity to $C_{n\alpha}$ is quite significant. When C is added it causes oscillation in α and β . The amplitudes

of α and β are not large, but the final values are different from those when $C_{n\alpha}$ =0, and they cause a series of aerodynamic data. The initial overshoots of β is about 4°.

The most important effects of $C_{n\alpha}$ on time history are in p, ϕ and r. Rolling speed becomes as large as 97.8 deg/sec after 20 seconds, which causes the aircraft to rotate more than four cycles about its X axis. Because of the unstable in roll degree of freedom, the vertical flight path angle γ comes up to -45° with related altitude loss 1620m. Meanwhile, Mach number is only increased in 0.073 because drag is strongly increased when α and β are very high. Generally speaking, the motion is similar to a typical spin.

The curve of heading angle shows a kind of non-linear oscillatory divergence.

According to the calculated results, we know that the motion almost displays a mirror image for positive and negative values of $C_{n\alpha}$. This phenomenon still exists when a derivative changes its sigh. By comparison, the effects of derivative $C_{n\dot{\alpha}}$ on time history are much smaller (fig.7). The response of α is almost no much difference with the situation $C_{n\dot{\alpha}}$ zeroed, and β only has a slight oscillation. The bank angle ϕ maintains about 60 degree. The flight path angle γ comes up to about 20 degree in 20 seconds. The aircraft motion is a kind of turn with descent. The altitude loss is not so large (808m. in 20 seconds), but the gain of Mach number is as high as 0.105 because of very little drag increasing. Because of the bank angle, the heading angle ψ keeps increasing and reaches -66°. That is quite different from the effects of $C_{n\alpha}$ on ψ.

The effects of derivative C_{nq} on time history is somewhat similar to the effects of $C_{n\alpha}$, but the motion process is relatively mild and slow. The time history figures are omitted. The effects of the acceleration derivative $C_{n\dot{\beta}}$ on time history are too small to be presented graphically and can also be completely omitted.

It is understandable that the effects of combination of $C_{n\alpha}$, $C_{n\dot{\alpha}}$, C_{nq} and $C_{n\beta}$ on time history are extremely significant. The aircraft motion presents a serious divergence when this combination is considered. The calculated results and figures are not presented here.

Effects of $C_{l\alpha}$, $C_{l\dot{\alpha}}$, C_{lq}, $C_{l\dot{\beta}}$

Since no applicable data for derivative $C_{n\alpha}$ is known for the aircraft used in this paper, we assume $C_{n\alpha}$ = 0.05, which are data for another aeroplane with 70° swept angle. The inconsistency has to be accepted in this case.

In our example, $C_{l\alpha}$ has very strong effects on aircraft response and causes a serious unstable motion. From the calculated results we know that the effects on motion are not exactly symmetrical when $C_{l\alpha}$ changes its values from positive to negative. this is owing to the unsymmetrical behavior of curve C_l-α when β=0. Generally speaking, the aircraft motion is a kind of spin in this example when $C_{l\alpha}$ is considered. Again the calculated results are omitted.

The motion sensitivity to derivatives $C_{l\dot{\alpha}}$ and C_{lq} is quite significant. An oscillatory divergence of motion occurs when $C_{l\dot{\alpha}}$ or C_{lq} is considered and that causes strong oscillation in β, p, q and r . In both cases, bank angle ϕ becomes very high and the aircraft turns into dive, which makes the aircraft lose its altitude and increase its Mach number very fast.

The motion sensitivity to $C_{l\dot{\beta}}$ is so small that can be neglected.

The effects of combination of $C_{l\alpha}$, $C_{l\dot{\alpha}}$, C_{lq} and $C_{l\beta}$ on time history are also significant. The results are not presented here.

Effects of C_{mp}, $C_{m\gamma}$ and $C_{m\dot{\beta}}$

The effects of C_{mp}, $C_{m\gamma}$ and $C_{m\dot{\beta}}$ on time history are insignificant and are too small to be presented graphically. The results are also omitted.

Conclusion

1. In order to analyse the high angles-of-attack flight dynamic behaviors of high manoeuvre performance aircraft, the nonlinear models should be used. We must analyse not only the local stability around an equilibrium point but also the global stability.

2. According to the O.D.E. qualitative theory, the commonly used design criteria for predicting departure characteristics and spin susceptibility are only the simplified results of local stability at equilibrium point. Although they are not perfect, the example shows that the criteria are still available in the stall region.

3. The variance of local stability at equilibrium surface can be used to identify the important phenomena of high angle-of-attack flight, such as, wing rock, departure and spin.

4. Among the cross-coupling derivatives, the lateral moment derivatives due to pitching are more important than the pitching moment derivatives due to rolling and yawing. The derivatives which cause the strongest effects on aircraft behavior are $C_{n\alpha}$, $C_{l\alpha}$, $C_{l\dot{\alpha}}$. The derivatives $C_{n\dot{\alpha}}$, C_{nq} and C_{lq} are also important. So it is very important to prevent unsymmetrical vortex separation on wing or fuselage. The effects of C_{mp}, $C_{m\gamma}$, $C_{m\dot{\beta}}$ and $C_{n\dot{\beta}}$ are generally insignificant.

5. When each derivative or combination which has strong effects on

time history and cause instability is taken into account, the aircraft responses in our example might be classified into two types.

a. The motion of the aircraft is similar to spin with large p and r and high α (sometimes high β as well) and a fast and continual increasing in ϕ . In this case, the altitude loss may be very large but the gain of Mach number is relatively small. The typical examples of this kind of motions is presented in fig. 6.

b. The aircraft motion is similar to turn with fast altitude loss. The angles α and β are not so high and bank angle ϕ usually keeps a certain value instead of increasing continuously. In this case, the altitude loss is large, and the increasing of Mach number may be large as well. The typical example is presented in fig.7.

6. In general, for positive and negative values of lateral derivatives which are caused by longitudinal parameters, the motion of aircraft usually displayed a mirrow image, but sometimes some difference may exist.

7. The magnitude of the cross-coupling derivatives may strongly vary with the aircraft configuration, Mach number and other factors. So the present results, although are probably representative of a modern fighter flying at high enough angles of attack to cause asymmetric flow conditions, should not automatically be generalized.

References

(1) Mehra,R.K. et.al.
AD-A051850 (1977)

(2) Mehra,R.K., Carroll,J.V.
Rep. ONP-CR215-248-2 (1978)

(3) Mehra,R.K., Carroll,J.V.
AIAA PAPER (80-1599)

(4) Carroll,J.V. , Mehra,R.K.
AIAA Paper (1982)

(5) Zagaynov,G.I., Guman,G.I.
ICAS (84-421)

(6) Kalvists,J.
AGARD CP-235 (1978)

(7) Skow,A.M., Erickson.G.E.
AGARD High-Angles-of-Attack Aerodyn. Meeting., Dec. (1982).

(8) Malcolm, G.N.
AGARD LS 114, Paper 15, (1981).

(9) Coe, P.L.Jr, Graham, A.B.Chamber, J.R. NASA TN D-7972, (1975).

(10) Orlik-Ruckemann,K.J.
AGARD LS 114, Paper 15, (1981).

(11) Curry, W.H. Orlik-Ruckemann, K.J.
AGARD CP 235, Paper 24. (1978).

(12) Fox, C.H.Jr., Lamar, J.E.
NASA TN D-7651, (1974).

(13) Shanks, R.E.
NASA TN D-1822, (1963)

(14) Kalviste, J.
AGARD CP 235, Paper 29, (1978).

(15) Barker, L.E.Jr., Bowtes,R.L., Williams,L.H. NASA TN D-7347, (1973)